Velocity and enthalpy distributions in the compressible turbulent boundary layer on a flat plate

By D. A. SPENCE
Royal Aircraft Establishment, Farnborough†

(Received 1 November 1959)

The object of this paper is to present a unified account of the distributions of velocity, shear stress and enthalpy in the compressible turbulent boundary layer on a flat plate. As a start, the set of velocity profiles measured over a range of heat-transfer conditions at Mach numbers between 5 and 8 by Lobb, Winkler & Persh (1955) is examined. It is found that by plotting in terms of the Howarth variable $\eta = \int_0^y (\rho/\rho_0)\,dy$, the outer parts of the profiles for different Mach numbers are brought together on a single curve of the approximate form $u/u_\infty = (\eta/\Delta)^{1/n}$, Δ being the transformed boundary-layer thickness. By evaluating the reference density ρ_0 and kinematic viscosity ν_0 at the so-called 'intermediate' enthalpy (Eckert 1955) the inner parts of the profiles can also be collapsed, although less completely, to fit a 'law of the wall' $u/u_\tau = A \log(\eta u_\tau/\nu_0 - c) + B$. Here $u_\tau = (\tau_w/\rho_0)^{\frac{1}{2}}$, and A, B and c are the same constants as in incompressible flow.

These properties provide a physical starting point from which the remaining features of the mean flow can be calculated. By substitution of appropriate stream functions in the equation of motion the distribution of shear stress τ in inner and outer regions is found; this approximates to the form

$$\tau/\tau_w = 1 - (u/u_\infty)^{n+2}$$

over the whole layer. A relation between the distributions of enthalpy and shear stress is then found from the energy equation, using a turbulent Prandtl number α which is assumed constant across the layer to relate eddy conductivity to eddy viscosity. The final expression is similar in form to Crocco's integral for the laminar boundary layer with α taking the place of the laminar Prandtl number σ, but contains two extra terms proportional respectively to $(\alpha - \sigma)c_f$ and $(\alpha - \sigma)c_f^{\frac{1}{2}}$, which represent the effect of the inner viscous regions.

The enthalpy integral is evaluated using the stated velocity-shear relation, and an expression which agrees well with the available experimental data is found for the heat-transfer coefficient as a function of recovery factor and skin-friction coefficient. It is also found that the usual quadratic enthalpy-velocity relation, exact for $\alpha = \sigma = 1$, remains an acceptable approximation for Prandtl numbers considerably different from unity.

---

† At Cornell University, Ithaca, New York, 1959–60.

1. Introduction

1.1. *Howarth's transformation*

A number of recent authors on the compressible turbulent boundary layer have noticed that, as in the laminar case, the analysis can be greatly simplified by using instead of the physical co-ordinate y the variable

$$\eta = \int_0^y (\rho/\rho_0)\, dy \tag{1}$$

introduced by Howarth. Here ρ is the density at height y above the surface, and ρ_0 an arbitrarily chosen reference density. For the laminar boundary layer on a flat plate, if the product $\rho\mu$ of density and viscosity is treated as constant, the effect of the transformation is to free the velocity profiles of explicit dependence on Mach number and Prandtl number. They can be written

$$u/u_\infty = f(\eta/\Delta), \tag{2}$$

where f is a universal function, u_∞ is the free-stream velocity at the outer edge of the boundary layer, and Δ is the transformed value of a suitably-defined boundary-layer thickness δ.

It seems natural to ask whether any property like this may also hold for velocity profiles in the turbulent case. In an attempt to answer this question, a set of profiles measured by Lobb *et al.* (1955) is examined in the present paper. These were obtained at Mach numbers between 5 and 8, and momentum-thickness Reynolds numbers R_θ between 5000 and 12,500, with varying amounts of heat transfer. When plotted in the form of u/u_∞ against y/δ as in figure 6 the profiles are widely different, but the transformation (1) almost eliminates the scatter, so that in figure 7 all lie close to a single curve. Except near the inner and outer limits, the power law

$$u/u_\infty = (\eta/\Delta)^{1/n} \tag{3}$$

with $n = 9$ provides a good interpolation to the curve, and from experience of incompressible boundary layers one would expect the index $1/n$ to decrease slowly with increasing R_θ over a wider range.

This particular form of interpolation has of course no special physical significance, but it does make the calculation of the remaining properties of the mean flow fairly straightforward. Most recent workers on the incompressible boundary layer have preferred to express the outer velocity distribution in terms of the 'defect' or 'wake' laws elegantly formulated by Clauser (1956) and Coles (1956). These laws offer more insight into the physical processes at work in transferring turbulent energy through successive eddy scales within the boundary layer, but in the zero-pressure gradient case they have little advantage in accuracy over the simpler type of law used here. Dimensional analysis shows that the incompressible boundary-layer profile on a flat plate can depend on two parameters only; in the outer part one of these must be y/δ, and no generality is lost in using for the second the index $1/n$ of the interpolating power law, which clearly depends on R_θ.

1.2. *Law of the wall*

The form of equation (2) is, however, inappropriate in the sublayer and inner turbulent core, for we know that in incompressible flow the velocity distribution

in these regions is given by the 'law of the wall'. That is, the velocity ratio u/u_τ, where u_τ is the friction velocity $(\tau_w/\rho)^{\frac{1}{2}}$, is a universal function of yu_τ/ν. This could only be strictly true if the boundary-layer thickness were infinite, but its approximate validity at finite Reynolds numbers is established beyond doubt, and one is naturally led to try to generalize the law for compressible flows.

A way of doing this is suggested by the form of the sublayer profile. If the friction velocity is defined for a compressible flow in terms of the reference density by

$$\tau_w = \rho_0 u_\tau^2, \tag{4}$$

then, since the shear stress $\mu(\partial u/\partial y)$ in the sublayer is nearly constant and equal to τ_w, the profile may be written

$$\frac{u}{u_\tau} = \frac{\tau_w}{u_\tau}\int_0^y \frac{dy}{\mu} = \eta u_\tau/\nu_0. \tag{5}$$

Here $\nu_0 = \mu_0/\rho_0$, and it has been assumed as before that $\rho\mu$ is constant. The accuracy of this assumption is discussed in §7. Equation (5) is of the form

$$\frac{u}{u_\tau} = g(\eta u_\tau/\nu_0) \tag{6}$$

and by analogy with the incompressible case one might expect an expression of this form to hold also in the buffer layer and in the turbulent core. To agree with the well-known expression for incompressible flow, g would have to approach the form $A\log(\eta u_\tau/\nu_0)+B$ in the fully turbulent core, i.e. for $\eta u_\tau/\nu_0 > 30$ say. If, in addition, the physically realistic requirement of a continuous derivative, i.e. of continuous viscous shear stress, at the intersection with the sublayer profile (5) is imposed, we are led to the compressible version of an expression derived by Squire (1948), namely

$$\frac{u}{u_\tau} = A\log\left(\frac{\eta u_\tau}{\nu_0} - c\right) + B \tag{7}$$

in which A and B have the accepted values 2·5, 5·5, respectively, and $c = 5{\cdot}3$. With these values the intersection of (5) and (7) is at $\eta u_\tau/\nu_0 = 7{\cdot}8$.

1.3. *Choice of the reference density*

The outer velocity distribution (2) is independent of ρ_0, but that defined by (6) does depend on the particular reference density which is chosen. A way of deciding on the appropriate value is suggested by the 'intermediate enthalpy' method of correlating compressible and incompressible values of the skin fraction. It has been found experimentally—for example, by Matting, Chapman, Nyholm & Thomas (1959)—that the wall shearing stress τ_w a distance x downstream of the virtual origin of turbulence in a compressible boundary layer can be written $\frac{1}{2}\rho_m u_\infty^2 c_f(u_\infty x/\nu_m)$, where c_f is the same function of the Reynolds number as in incompressible flow. The suffix m now denotes evaluation of the physical quantities at a certain intermediate value h_m of the enthalpy, for which Eckert (1955) has given the empirical equation

$$h_m = 0{\cdot}5(h_w+h_\infty) + 0{\cdot}22(h_r-h_\infty), \tag{8}$$

where suffixes w, ∞ and r refer to wall, free stream and recovery (i.e. zero heat transfer) values.

But the velocity distributions (3) and (7) alone contain enough information for the skin friction to be deduced, and it is shown in § 2 that if the two laws join with $\partial u/\partial y$ continuous, then

$$\tau_w/\rho_0 u_\infty^2 = C(\rho_\infty u_\infty \theta/\mu_0)^{-2/(n+1)} = D(u_\infty x/\nu_0)^{-2/(n+3)}, \tag{9}$$

where $C(n)$ and $D(n)$ have almost exactly the values used in the recognized incompressible power-law formulae. The fact that the power-law formulae for skin friction can be derived *a priori* in this way does not seem to be well known: most authors have regarded the formulae, at least for the cases $n = 9$ and $n = 11$, merely as interpolations to more complicated expressions of the Karman–Schoenherr type, which were originally derived by use of a velocity-defect law. But if ρ_0 and μ_0 are the values which apply at Eckert's intermediate enthalpy h_m, then (9) gives precisely the value of skin friction predicted when his law is used to generalize the latter formulae to compressible flow. It follows, therefore, that if we set

$$\rho_0 = \rho_m, \quad \mu_0 = \mu_m, \tag{10}$$

the inner law (6) is consistent with the known variation of skin friction with Mach number. These reference values are therefore used in the remainder of the paper.

1.4. *Distributions of shear stress and enthalpy*

Before comparing the velocity laws (3) and (7) directly with the available experimental profiles, it is useful to calculate the distributions of shear stress and enthalpy across the layer on the assumption that they do in fact hold. The shear stress is found in § 3, using the equations of motion in conjunction with appropriate forms of the steam function in inner and outer regions. General expressions involving only the functional forms of the velocity profile are found first, but on inserting the precise distributions (3) and (7) an approximate expression is obtained for τ/τ_w in terms of u/u_∞ alone. This is required in § 4, where a turbulent analogue of Crocco's integral relating the enthalpy distribution to those of shear stress and velocity is derived from the energy equation.

The derivation calls for some further knowledge of the turbulent transport mechanism, in addition to that implied by the distribution of velocity (from which those of shear stress and therefore of eddy viscosity followed). For this purpose it is assumed, following van Driest (1955) and Rubesin (1953), that the ratio of diffusivities of momentum and heat due to the turbulent motion is constant across the layer. This ratio defines a turbulent Prandtl number α, different in general from the laminar value σ which corresponds to molecular transport mechanisms. Rubesin and van Driest had recourse to mixing length theories to provide the distribution of shear stress, but we can now use the distribution obtained directly from the velocity profile. Both this and the distribution of enthalpy to which it leads are therefore consistent with the equations of continuity, momentum and energy, and with each other. This was not the case with those obtained by previous authors.

1.5. *Recovery factor and heat-transfer coefficient*

From the enthalpy distribution, expressions are found in §5 for the recovery factor (i.e. the fraction of the kinetic energy of the free stream which is recovered as enthalpy at an adiabatic wall) and for the heat-transfer coefficient. In each, the more important term depends only on α, but correction terms proportional to $(\alpha-\sigma)(\rho_\infty c_f/\rho_m)$ and to $(\alpha-\sigma)(\rho_\infty c_f/\rho_m)^{\frac{1}{2}}$, respectively, appear. The value of α cannot be obtained directly from experiments, but it is possible to infer a value from that of the recovery factor, which can be measured. The value of α so found can then be used to predict the heat-transfer coefficient which corresponds to a particular recovery factor. The resulting heat-transfer coefficients lie well within the range which would have been expected from experiments.

Finally, in §6, the experimental velocity profiles referred to are examined to show their compatibility with the model of the boundary layer which has been elaborated in the paper.

2. Expression for skin friction

As remarked in §1.3, an expression for skin friction can be derived directly from those for the inner and outer velocity profiles, on the assumption that the gradient $\partial u/\partial\eta$ is continuous at their intersection. Using (2), (6) and writing $\eta u_\tau/\nu_0 = \zeta$, we should have at this point

$$\frac{u}{u_\infty} = f\left(\frac{\zeta\nu_0}{u_\tau\Delta}\right) = \frac{u_\tau}{u_\infty}g(\zeta),$$

$$\frac{1}{u_\infty}\frac{\partial u}{\partial\zeta} = \frac{\nu_0}{u_\tau\Delta}f'\left(\frac{\zeta\nu_0}{u_\tau\Delta}\right) = \frac{u_\tau}{u_\infty}g'(\zeta).$$

Eliminating ζ between these two equations clearly yields a relation between u_τ/u_∞ and $u_\tau\Delta/\nu_0$ or, what is the same thing, between $(u_\tau/u_\infty)^2$ and $u_\infty\Delta/\nu_0$. In particular, the power law (3) can be rewritten

$$\frac{u}{u_\tau} = \left(\frac{u_\tau}{u_\infty}\right)^{-(n+1)/n}\left(\frac{u_\infty\Delta}{\nu_0}\right)^{-1/n}\zeta^{1/n} = K\zeta^{1/n} \tag{11}$$

say, whence

$$\frac{\tau_w}{\rho_0 u_\infty^2} = \left(\frac{u_\tau}{u_\infty}\right)^2 = K^{-2n/(n+1)}\left(\frac{u_\infty\Delta}{\nu_0}\right)^{-2/(n+1)}. \tag{12}$$

Applying the second condition that $\partial u/\partial\zeta$ is continuous at the intersection of (11) with the logarithmic law (7) (from which c can be omitted since the join occurs at values of ζ much greater than 5·3), K is found explicitly as

$$K = nA\exp[(B/nA)-1]. \tag{13}$$

The values of K for $n = 7$, 9, 11 are tabulated in table 1, and the corresponding outer curves are plotted against ζ in figure 1. The fact that the power and logarithmic laws in each case lie close together for a fair distance on either side of the point of contact shows the joining condition to have been a realistic one.

The momentum thickness may be evaluated using the power law (3), since integration smooths out errors produced by the departure of the profile from this form at the inner and outer edges; we obtain

$$\theta = \int_0^\delta (\rho u/\rho_\infty u_\infty)\,(1-u/u_\infty)\,dy = \{n/(n+1)\,(n+2)\}\,(\rho_0\Delta/\rho_\infty). \tag{14}$$

n	K	$2/(n+1)$	C	C'	Range of R_θ
7	8·82	$\frac{1}{4}$	0·0124	0·0130	100–5000
9	10·57	$\frac{1}{5}$	0·0087	0·0088	500–50,000
11	12·36	$\frac{1}{6}$	0·00645	0·00655	3000–600,000

TABLE 1. Power laws for incompressible skin friction

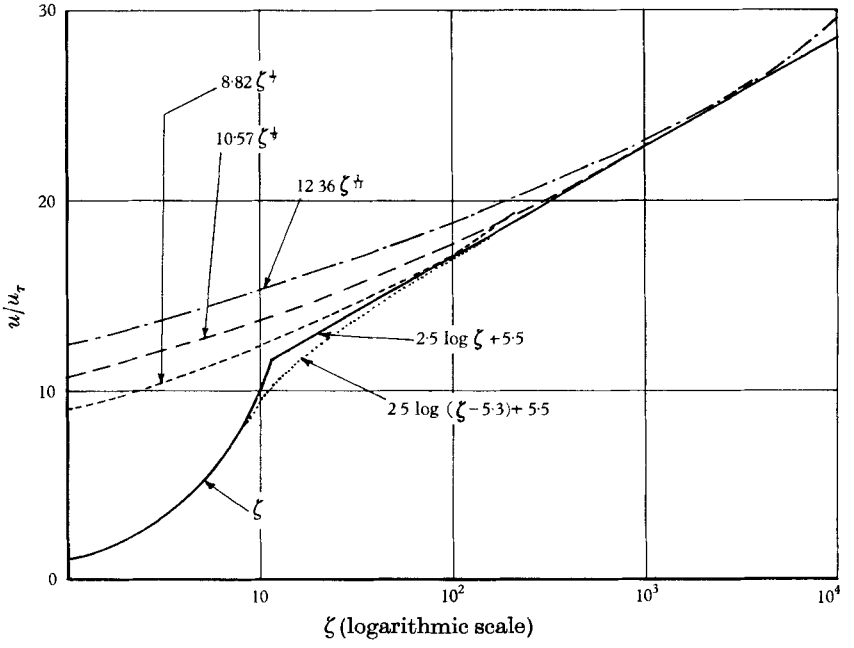

FIGURE 1. Various 'inner' velocity laws.

Replacing Δ in (12) by this value of θ yields the first of the expressions (9) for skin friction. The second, in terms of a Reynolds number based on x, follows it by writing the integral momentum equation as

$$d(\rho_\infty u_\infty \theta/\mu_m)/d(u_\infty x/\nu_m) = (u_\tau/u_\infty)^2$$

and setting $\theta = 0$ when $x = 0$ after integration. The constants C and D are related to K by

$$(n+1)\,C^{\frac{1}{2}(n+1)} = (n+3)\,D^{\frac{1}{2}(n+3)} = n(n+2)^{-1}K^{-n}.$$

The values of C obtained using K from (13) in this relation are listed in table 1, together with values C' corresponding to the accepted incompressible power-law expressions $\frac{1}{2}c_f = C'R_\theta^{-2/(n+1)}$ given in the three cases by von Kármán (1921), Young (1953) and Falkner (1943). The ranges of applicability of the incompressible laws are those suggested by Culick & Hill (1958).

The agreement between the value of C found by the method just described and the accepted value C' is close for the $\frac{1}{5}$th and $\frac{1}{6}$th power-laws, and within 5% for the quarter power-law which holds at the lowest Reynolds number. With slightly different values of K (8·85, 10·50, 12·23, respectively) C could be made to agree exactly with C'. The corresponding power-law velocity curves would still approximate closely to the logarithmic expression over a considerable range of R_θ and might just as well have been chosen in the first place instead of those given by (13).

3. Shear-stress distribution

The equations of continuity and motion are

$$\frac{\partial}{\partial x}(\rho u)+\frac{\partial}{\partial y}(\rho v+\overline{\rho' v'}) = 0, \tag{15}$$

$$\rho u\frac{\partial u}{\partial x}+(\rho v+\overline{\rho' v'})\frac{\partial u}{\partial y} = \frac{\partial \tau}{\partial y}, \tag{16}$$

respectively, where primes denote turbulent fluctuations, bars the time means of their products, and

$$\tau = \mu\frac{\partial u}{\partial y}-\rho\overline{u'v'}$$

is the shear stress. In view of (15) a stream function ψ may be defined by writing

$$\rho_m\frac{\partial \psi}{\partial y} = \rho u, \quad -\rho_m\frac{\partial \psi}{\partial x} = \rho v+\overline{\rho' v'}. \tag{17}$$

Different forms for ψ are appropriate in the inner and outer regions, which we now treat in turn.

3.1. *Inner region*

The stream function may be written

$$\psi = \nu_m G\left(\frac{\eta u_\tau}{\nu_m}\right) = \nu_m G(\zeta) \tag{18}$$

say. Then

$$g(\zeta) = \frac{u}{u_\tau} = G'(\zeta)$$

and (treating ν_m as independent of x, i.e. for a constant temperature wall) the momentum equation (16) becomes

$$-\rho u^2\lambda(x) = \frac{\partial \tau}{\partial y}, \tag{19}$$

where $\lambda(x) = -(d/dx)\log(u_\tau/u_\infty)$. This is the compressible flow version of an expression found in an earlier paper (Spence 1951). On integration

$$\tau/\tau_w = 1-(\nu_m/u_\tau)\lambda(x)\int_0^\zeta [g(\zeta_1)]^2\,d\zeta_1. \tag{20}$$

Thus with a knowledge of the universal function g in equation (6) and of the

variation of τ_w with x, the shear stress in the inner part of the layer may be found from (19). The result of integrating the logarithmic expression (7) can be written

$$\int_0^\zeta g^2 d\zeta = \zeta g^2\{1 - Ag^{-1} + O(g^{-2})\}$$

so that for large enough values of $g = u/u_\tau$,

$$\tau/\tau_w \doteqdot 1 - (\nu_m/u_\tau)\,\lambda(x)\,\zeta\left(\frac{u}{u_\tau}\right)^2 = 1 - \lambda(x)\,\eta\left(\frac{u}{u_\tau}\right)^2. \tag{21}$$

3.2. *Outer region*

The velocity law (2) may be written in terms of a stream function

$$\psi = u_\infty \Delta F(\eta/\Delta) = u_\infty \Delta F(\xi) \tag{22}$$

say. In this case $$f(\xi) = \frac{u}{u_\infty} = F'(\xi)$$

and the momentum equation can be written

$$-\Lambda F(\xi)\,F''(\xi) = (\rho_m \Delta/\rho\tau_w)\frac{\partial \tau}{\partial y} = \frac{\partial}{\partial \xi}\left(\frac{\tau}{\tau_w}\right), \tag{23}$$

where $\Lambda = (\rho_m u_\infty^2/\tau_w)\,(d\Delta/dx)$ may be supposed known. F contains a constant of integration which should strictly be evaluated by equating this value for $\partial\tau/\partial y$ to that given by (20) at the point of contact of the corresponding velocity laws, but as in determining θ/Δ, an adequate approximation is found simply by applying the outer law across the whole layer. Then by (22) $F(0) = 0$ since ψ must be constant on $\xi = 0$, and using the power-law velocity distribution we obtain $F(\xi) = \{n/(n+1)\}\,\xi^{1+1/n}$. Therefore, integrating (23),

$$1 - \frac{\tau}{\tau_w} = \xi^{1+2/n} = \xi\left(\frac{u}{u_\infty}\right)^2. \tag{24}$$

The coefficient of $\xi^{1+2/n}$ here has been set equal to unity in order to make τ/τ_w vanish at $\xi = 1$. The coefficient is actually $n\Lambda/(n+1)\,(n+2)$, which equals $(\rho_\infty u_\infty^2/\tau_w)\,(d\theta/dx)$ by (14), so this is a statement of the integral momentum equation.

The expression (24) is not very different from that which would have been found by using the inner law in the region where it applies, for logarithmic differentiation of (12) shows that

$$\lambda(x) = \{1/(n+1)\,\Delta\}\,(d\Delta/dx),$$

whence (21) may be written

$$1 - \frac{\tau}{\tau_w} = \frac{\Lambda}{n+1}\frac{\eta}{\Delta}\left(\frac{u}{u_\infty}\right)^2 = \left(1 + \frac{2}{n}\right)\xi\left(\frac{u}{u_\infty}\right)^2.$$

This is an approximation to (24) if $n \gg 1$.

Finally, (24) may be written in terms of velocity alone as

$$\frac{\tau}{\tau_w} = 1 - \left(\frac{u}{u_\infty}\right)^{n+2}, \tag{25}$$

in which form it will be used in the next section to evaluate the enthalpy distribution

4. Enthalpy distribution in terms of velocity and shear stress

The energy equation may be written

$$\rho u \frac{\partial h}{\partial x} + (\rho v + \overline{\rho' v'}) \frac{\partial h}{\partial y} = \frac{\partial q}{\partial y} + \tau \frac{\partial u}{\partial y}, \tag{26}$$

where h is the static enthalpy, and

$$q = \frac{k}{C_p} \frac{\partial h}{\partial y} - \rho \overline{v' h'}$$

is the heat flux per unit area towards the wall. In forming equation (26) triple products such as $\overline{u'^2 v'}$ have been excluded as is customary. Regarding h and q as functions of u, so that $\partial h/\partial x = (\partial u/\partial x)(dh/du)$, etc., and using the equation of motion (16), the left-hand side of (26) is seen to equal $(\partial \tau/\partial y)(dh/du)$. After dividing through by $\tau(\partial u/\partial y)$ the equation may therefore be written

$$\frac{1}{\tau}\frac{d\tau}{du}\frac{dh}{du} = \frac{1}{\tau}\frac{dq}{du} + 1. \tag{27}$$

An eddy viscosity ϵ and an eddy conductivity κ may now be defined by means of

$$-\rho \overline{u' v'} = \epsilon \frac{\partial u}{\partial y}, \quad -\rho \overline{h' v'} = \frac{\kappa}{C_p} \frac{\partial h}{\partial y}. \tag{28}$$

The laminar and turbulent Prandtl numbers are then

$$\sigma = \mu C_p / k, \quad \alpha = \epsilon C_p / \kappa,$$

respectively. In terms of these the ratio of the molecular contributions to q and τ is, say,

$$q_L/\tau_L = \left(\frac{k}{C_p}\frac{\partial h}{\partial y}\right) \Big/ \left(\mu \frac{\partial u}{\partial y}\right) = \frac{1}{\sigma}\frac{dh}{du},$$

and similarly that of the turbulent contributions (28) is

$$q_T/\tau_T = \frac{1}{\alpha}\frac{dh}{du}.$$

Combining the last two equations,

$$q = q_L + q_T = \left(\frac{\tau_L}{\sigma} + \frac{\tau_T}{\alpha}\right)\frac{dh}{du} = \left\{\frac{\tau}{\alpha} + \left(\frac{1}{\sigma} - \frac{1}{\alpha}\right)\tau_L\right\}\frac{dh}{du}$$

and the energy equation (27) becomes

$$\frac{1}{\tau}\frac{d}{du}\left[\left\{\frac{\tau}{\alpha} + \left(\frac{1}{\sigma} - \frac{1}{\alpha}\right)\tau_L\right\}\frac{dh}{du}\right] - \frac{1}{\tau}\frac{d\tau}{du}\frac{dh}{du} = -1. \tag{29}$$

So far it has not been necessary to make any physical assumptions, and equation (29) is exact. To proceed further we may suppose both σ and α are constant across the layer. The accepted value of σ is about 0·7 for air up to about 1000 °K, and a value of about 0·85 for α will be inferred in §5 from the known values of recovery factor.

4.1. *Integration of the energy equation*

The fact that the viscous contribution to shear stress falls off very rapidly with distance from the wall—in fact exponentially with velocity, decreasing almost to zero in a region of the turbulent core where the total stress is still not much less than τ_w—makes it possible to integrate the last equation in a simple manner. After multiplication through by $\tau^{1-\alpha}$, the equation can be written

$$\frac{d}{du}\left(\tau^{1-\alpha}\frac{dh}{du}\right)+\alpha\tau^{1-\alpha}=-\beta\tau^{-\alpha}\frac{d}{du}\left(\tau_L\frac{dh}{du}\right), \tag{30}$$

where $\beta=(\alpha/\sigma)-1$. In the region where $\tau_L \neq 0$, τ may be treated as constant and equal to τ_w on the right-hand side. Then integrating

$$\left(\frac{\tau}{\tau_w}\right)^{1-\alpha}\frac{dh}{du}-\left(\frac{dh}{du}\right)_w+\alpha\int_0^u\left(\frac{\tau}{\tau_w}\right)^{1-\alpha}du=-\beta\left\{\frac{\tau_L}{\tau_w}\frac{dh}{du}-\left(\frac{dh}{du}\right)_w\right\} \tag{31}$$

and re-arranging,

$$\frac{dh}{du}=\left(\frac{\tau}{\tau_w}\right)^{\alpha-1}\left\{\frac{\alpha}{\sigma}\left(\frac{dh}{du}\right)_w-\int_0^u\left(\frac{\tau}{\tau_w}\right)^{1-\alpha}du\right\}\left\{1-\beta\left(\frac{\tau}{\tau_w}\right)^{\alpha-1}\left(\frac{\tau_L}{\tau_w}\right)+O(\beta^2)\right\}. \tag{32}$$

The result of integrating (32) with respect to u, treating τ again as equal to τ_w in the term involving τ_L, may be written, excluding $O(\beta^2)$, as

$$h(u)-h_w=\frac{u_\infty}{\sigma}\left(\frac{dh}{du}\right)_w\left\{I(f)-(\alpha-\sigma)\frac{u_\tau}{u_\infty}L(g)\right\}-u_\infty^2\left\{K(f)-(\alpha-\sigma)\left(\frac{u_\tau}{u_\infty}\right)^2N(g)\right\}, \tag{33}$$

where for convenience f and g have been written for u/u_∞ and u/u_τ, respectively, and

$$\left.\begin{aligned} I(f)&=\alpha\int_0^f\left(\frac{\tau}{\tau_w}\right)^{\alpha-1}df_1,\\ K(f)&=\alpha\int_0^f\left(\frac{\tau}{\tau_w}\right)^{\alpha-1}df_1\int_0^{f_1}\left(\frac{\tau}{\tau_w}\right)^{1-\alpha}df_2\end{aligned}\right\} \tag{34}$$

and

$$L(g)=\int_0^g\frac{\tau_L}{\tau_w}dg,\quad N(g)=\int_0^g\frac{\tau_L}{\tau_w}g\,dg. \tag{35}$$

On setting $\alpha=\sigma$, we are left in (33) with the well-known Crocco integral for the enthalpy distribution in the laminar boundary layer at zero pressure gradient (which could also have been obtained at once from (32)). To evaluate the last two integrals we may set $\tau_L=\tau_w$ in the sublayer, and obtain the value of $\tau_L=\mu(\partial u/\partial y)$ in the buffer layer by differentiating (7) with $\rho\mu$ constant; this yields

$$\tau_L/\tau_w=1,\quad \exp\left(-\frac{g-\zeta_1}{A}\right),$$

according as $u/u_\tau = g \lesseqgtr \zeta_1 (= 7{\cdot}8)$. Then for $g > \zeta_1$,

$$L = L_0 - \frac{\tau_L}{\tau_w} A, \quad N = N_0 - \frac{\tau_L}{\tau_w} A(g + A), \tag{36}$$

where $$L_0 = \zeta_1 + A = 10{\cdot}3, \quad N_0 = \tfrac{1}{2}L_0^2 + \tfrac{1}{2}A^2 = 56{\cdot}2.$$

Except in the innermost part of the turbulent core we may set $\tau_L/\tau_w = 0$ and simply use the latter values. Values fairly close to these can also be obtained from other recognized interpolations for the buffer-layer profile; for instance, Rannie (1956) has suggested the formula

$$\frac{u}{u_\tau} = (1/\sqrt{\kappa_1}) \tanh (\zeta \sqrt{\kappa_1})$$

with $1/\sqrt{\kappa_1} = 14{\cdot}53$, for incompressible flow in the region $0 < \zeta < 27{\cdot}8$. The corresponding value of τ_L/τ_w is $1 - \kappa_1 (u/u_\tau)^2$, and by integrating up to the point where this vanishes we find $L_0 = 9{\cdot}7$, $N_0 = 52{\cdot}8$. (The less accurate assumption of an abrupt laminar-turbulent interface without a buffer layer at the point where $\zeta = A \log \zeta + B$, i.e. at $\zeta = 11{\cdot}7$, gives $L_0 = 11{\cdot}7$, $N_0 = 68{\cdot}5$.)

4.2. *Recovery factor and heat-transfer coefficient*

Since it gives the enthalpy at the outer edge of the boundary-layer equation (32) provides expressions for the recovery factor, i.e. the fraction of the kinetic energy of the external stream which is recovered as enthalpy at an insulated wall—and for the heat-transfer coefficient. With $u = u_\infty$, and introducing the skin-friction coefficient $c_f = \rho_m u_\tau^2 / \tfrac{1}{2}\rho_\infty u_\infty^2$, (32) becomes

$$h_\infty - h_w = \frac{u_\infty}{\sigma} \left(\frac{dh}{du}\right)_w \left\{ I(1) - (\alpha - \sigma) L_0 \left(\frac{\rho_\infty}{\rho_m} \frac{c_f}{2}\right)^{\frac{1}{2}} \right\} - u_\infty^2 \left\{ K(1) - (\alpha - \sigma) N_0 \frac{\rho_\infty}{\rho_m} \frac{c_f}{2} \right\}. \tag{37}$$

In the case of zero heat transfer $(dh/du)_w = 0$, and h_w equals the recovery enthalpy h_r. The recovery factor is therefore

$$r = (h_r - h_\infty)/\tfrac{1}{2}u_\infty^2 = 2K(1) - \frac{\rho_\infty}{\rho_m} (\alpha - \sigma) N_0 c_f. \tag{38}$$

The inward heat flux at the wall per unit area when $h_w \neq h_r$ is

$$q_w = \left(\frac{k}{C_p} \frac{\partial h}{\partial y}\right)_w = \left(\frac{\mu}{\sigma}\right)_w \left(\frac{\partial u}{\partial y}\right)_w \left(\frac{dh}{du}\right)_w = \frac{\tau_w}{\sigma} \left(\frac{dh}{du}\right)_w.$$

Elimination of h_∞ from (37) and (38) shows that the first term on the right-hand side of (37) is equal to $h_r - h_w$. This value may be used to calculate the Stanton number, defined by

$$1/St = \rho_\infty u_\infty (h_r - h_w)/q_w = (2/c_f) I(1) - (2\rho_\infty/\rho_m c_f)^{\frac{1}{2}} (\alpha - \sigma) L_0. \tag{39}$$

For $\alpha = 1$ we should have $I(1) = 1$, and the right-hand side of (39) reduces for incompressible flow to the form $2/c_f - (2/c_f)^{\frac{1}{2}} \phi(\sigma)$ found by Rannie (1956). If also $\sigma = 1$ the equation becomes simply $St = \tfrac{1}{2}c_f$, which expresses the Reynolds analogy between heat and momentum transfer. In the general case, a Reynolds analogy factor may be defined by the ratio $St/\tfrac{1}{2}c_f$ as calculated from (39).

5. Evaluation of the enthalpy distribution

The distribution of shear stress in terms of velocity as given by (25) may now be used to evaluate the functions $I(f)$, $K(f)$ which occur in the enthalpy-velocity relationship (33). Writing f for u/u_∞, (25) is

$$\tau/\tau_w = 1-f^p,$$

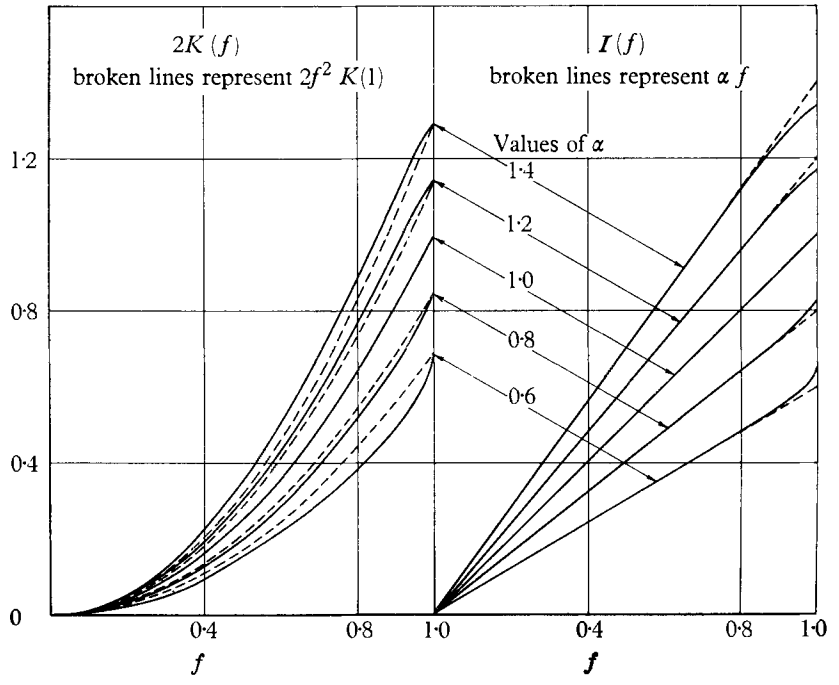

FIGURE 2. $I(f)$ and $2K(f)$ for several values of α ($p = 11$).

where $p = n+2$, and I and K, from (34), are

$$I(f) = \alpha\int_0^f (1-f_1^p)^{\alpha-1}\,df_1,$$

$$K(f) = \alpha\int_0^f (1-f_1^p)^{\alpha-1}\,df_1\int_0^{f_1}(1-f_2^p)^{1-\alpha}\,df_2.$$

These functions have been computed for $p = 9$, 11 and $\alpha = 0{\cdot}5(0{\cdot}1)1{\cdot}5$. $I(f)$ is an incomplete beta function, but the standard tables do not cover the required range of α and p; the functions were therefore found by quadrature after writing

$$(1-f)^{1-|1-\alpha|} = 1-z, \quad \left(\frac{1-f}{1-f^p}\right)^{|1-\alpha|} = i(z), \quad [(1-f)(1-f^p)]^{|1-\alpha|} = k(z).$$

Then for $\alpha < 1$

$$I(f) = \int_0^{z(f)} i(z_1)\,dz_1, \quad K(f) = \frac{1}{\alpha}\int_0^{z(f)} i(z_1)\,dz_1\int_0^{z_1} k(z_2)\,dz_2,$$

and for $\alpha > 1$

$$I(f) = \frac{\alpha}{2-\alpha}\int_0^{z(f)} k(z_1)\,dz_1, \quad K(f) = \frac{\alpha}{(2-\alpha)^2}\int_0^{z(f)} k(z_1)\,dz_1\int_0^{z_1} i(z_2)\,dz_2.$$

A check is provided by the fact that

$$I(1) = \alpha! \left(\frac{1}{p}\right)! \Big/ \left(\alpha + \frac{1}{p} - 1\right)!, \tag{40}$$

which can be found from tables.

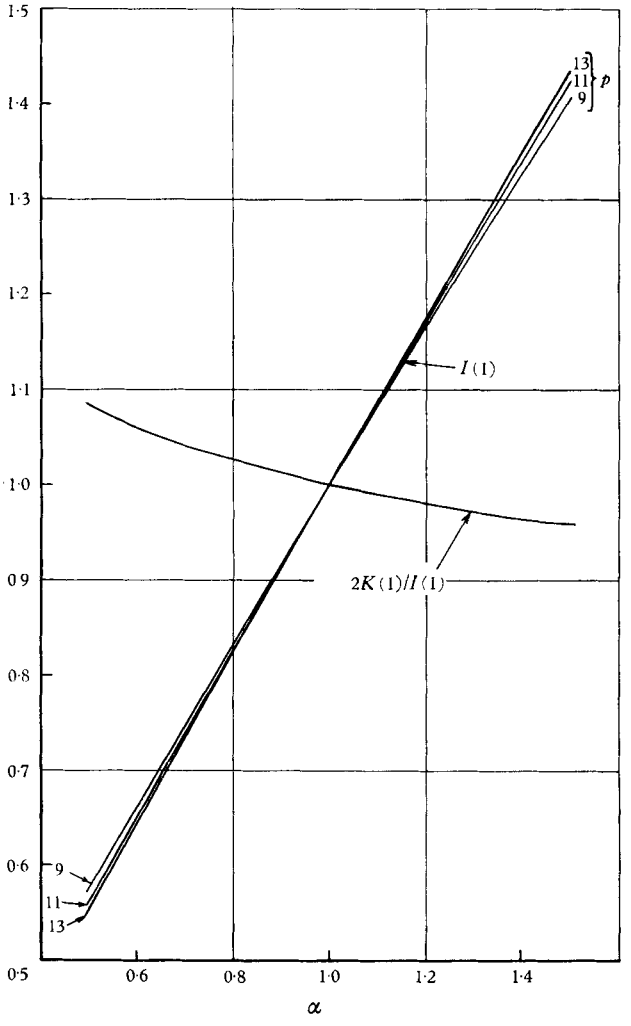

FIGURE 3. The values of $I(1)$ for $p = 9$, 11, 13, and $2K(1)/I(1)$ for $p = 11$.

Figure 2 shows the results for $\alpha = 0{\cdot}6$–$1{\cdot}4$ and $p = 11$ (i.e. for the $\frac{1}{9}$th power velocity profile). The broken lines representing αf and $f^2K(1)$ lie close in all cases to the curves of $I(f)$ and $K(f)$, respectively, and it follows that within the limits imposed by ignoring the terms involving c_f in (33), the enthalpy variation across the boundary layer can be well approximated by a quadratic in velocity, i.e. by

$$h(u) = h_w + (h_r - h_w)\frac{u}{u_\infty} - \tfrac{1}{2}ru^2 \tag{41}$$

over the range of Prandtl numbers (or recovery factors) covered by the computation.

Figure 3 shows the variation with α of $I(1)$. The curves for $p = 9$ and $p = 11$ lie very close together. A curve of $2K(1)/I(1)$ is also shown; in this case the results for $p = 9$ and $p = 11$ were indistinguishable. The variation of $2K(1)/I(1)$ is fairly slow, and its value can be read sufficiently accurately at non-tabular values of α

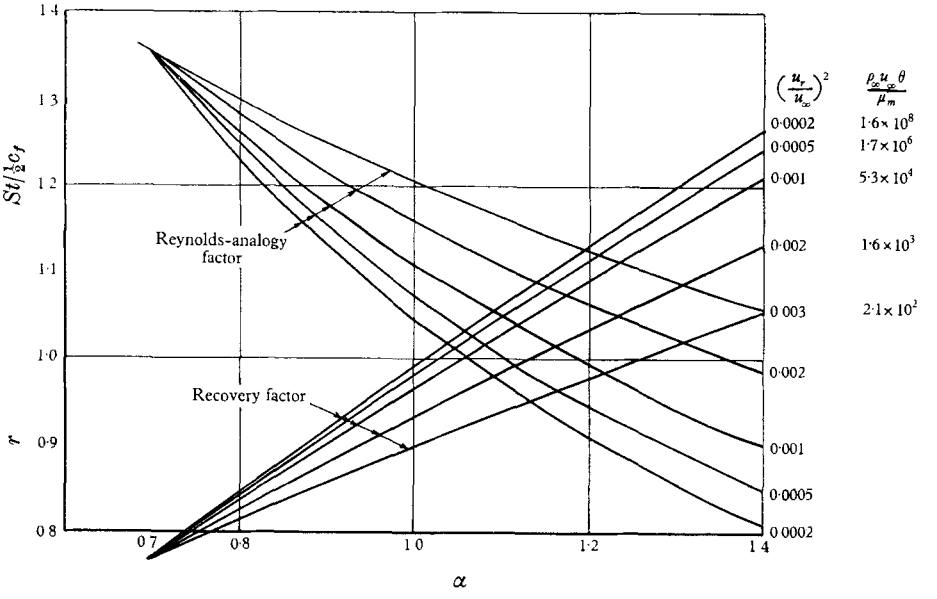

FIGURE 4. Variation of Reynolds analogy factor $St/\frac{1}{2}c_f$ and recovery factor r with α for several values of $(u_\tau/u_\infty)^2$ ($\sigma = 0{\cdot}7$).

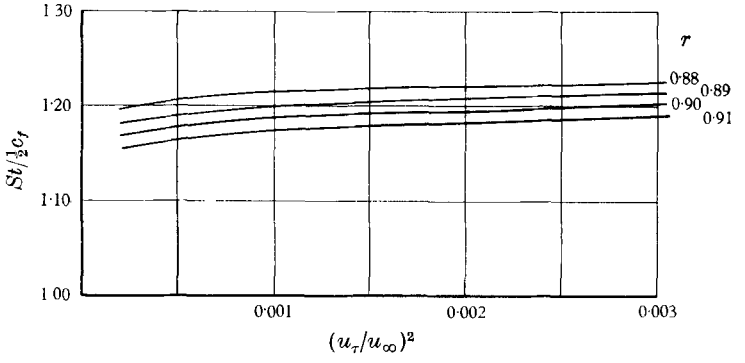

FIGURE 5. Variation of Reynolds analogy factor with $(u_\tau/u_\infty)^2$ for fixed values of recovery factor.

to permit accurate evaluation of $K(1)$, using the exact expression (40) for $I(1)$ at such values. A fairly wide range of Reynolds numbers is probably covered by the case $p = 11$; the values of $I(1)$ and $K(1)$ for this case have therefore been used to express the recovery and Reynolds analogy factors as functions of α for a number of values of $(u_\tau/u_\infty)^2$ (i.e. effectively of boundary layer Reynolds number $\rho_\infty u_\infty \theta/\mu_m$) in figure 4.

As was stated in § 1.5, values of α cannot be found directly from experiment. We do know, however, that for air at Mach numbers up to 8 the recovery factor r lies somewhere between 0·88 and 0·91. The curves of figure 4 have therefore been cross-plotted in figure 5 for constant values of r in this range, to show the variation of the Reynolds analogy factor with $(u_\tau/u_\infty)^2$. The actual magnitude of the factor $St/\frac{1}{2}c_f$ and its decrease when c_f decreases, i.e. when $\rho_\infty u_\infty \theta/\mu_m$ increases, are in good agreement with those found experimentally, which have been reviewed by Seiff (1954). The values of α in the cross-plot are in the range 0·85–0·9.

6. Experimental velocity profiles

6.1. *Outer law*

Figure 6 shows a set of profiles of u/u_∞ against y/δ measured by Lobb *et al.* (1955) at Mach numbers between 4·93 and 8·18 and stagnation temperatures near 300 °K. The $M = 8$ profiles lie near a $\frac{1}{5}$th power law, and those for $M = 5$ near a $\frac{1}{8}$th power law. The effect of the Howarth transformation is illustrated in figure 7 by plotting the profiles with η/Δ as the ordinate. This was found in terms of y/θ by writing

$$y = \int_0^\eta (h/h_m)\, d\eta \tag{42}$$

and using the quadratic enthalpy-velocity relationship (41) with $u/u_\infty = (\eta/\Delta)^{1/n}$. Integrating and inserting θ from (14), the relation

$$\eta/\Delta = (y/\theta)\,[a + b(u/u_\infty) - c(u/u_\infty)^2]^{-1} \tag{43}$$

is obtained, where

$$na = (n+1)\,(n+2)\,(h_w/h_\infty), \quad (n+2)\,b = (h_r - h_w)/h_\infty, \quad (n+1)\,c = (h_r/h_\infty) - 1.$$

The experimental values of y/θ, u/u_∞ and a, b, c (with $n = 9$) were used in (43). As plotted in figure 7 the profiles have collapsed almost entirely to a single curve lying close to the $\frac{1}{9}$th power law. This justifies the use that was made of the law in simplifying the integration with regard to η.

To avoid overcrowding the figure, only five of the profiles measured by Lobb *et al.* are shown. The same collapse to a single curve was, however, obtained with the remaining nine profiles as well.

6.2. *Law of the wall*

The inner parts of the same set of velocity profiles are plotted in the form of u/u_τ against $\eta u_\tau/\nu_m$ in figure 8, which also contains data from tests at the R.A.E. by Monaghan & Cooke (1953). The calculation of η from y by means of (42) is a little more complicated in this case, since it is necessary to take account of the dependence of the enthalpy distribution in the sublayer and buffer layer on τ_L/τ_w, as represented in (33) and (36). The details need not be given here.

The friction velocity was found from the experimental values of $\rho_\infty u_\infty \theta/\mu_m$, using the $\frac{1}{5}$th power-law formula for skin fraction in the form given by (9). The intermediate enthalpy was found from the wall and free-stream values, using Eckert's formula (8) and assuming a recovery factor $r = 0{\cdot}89$.

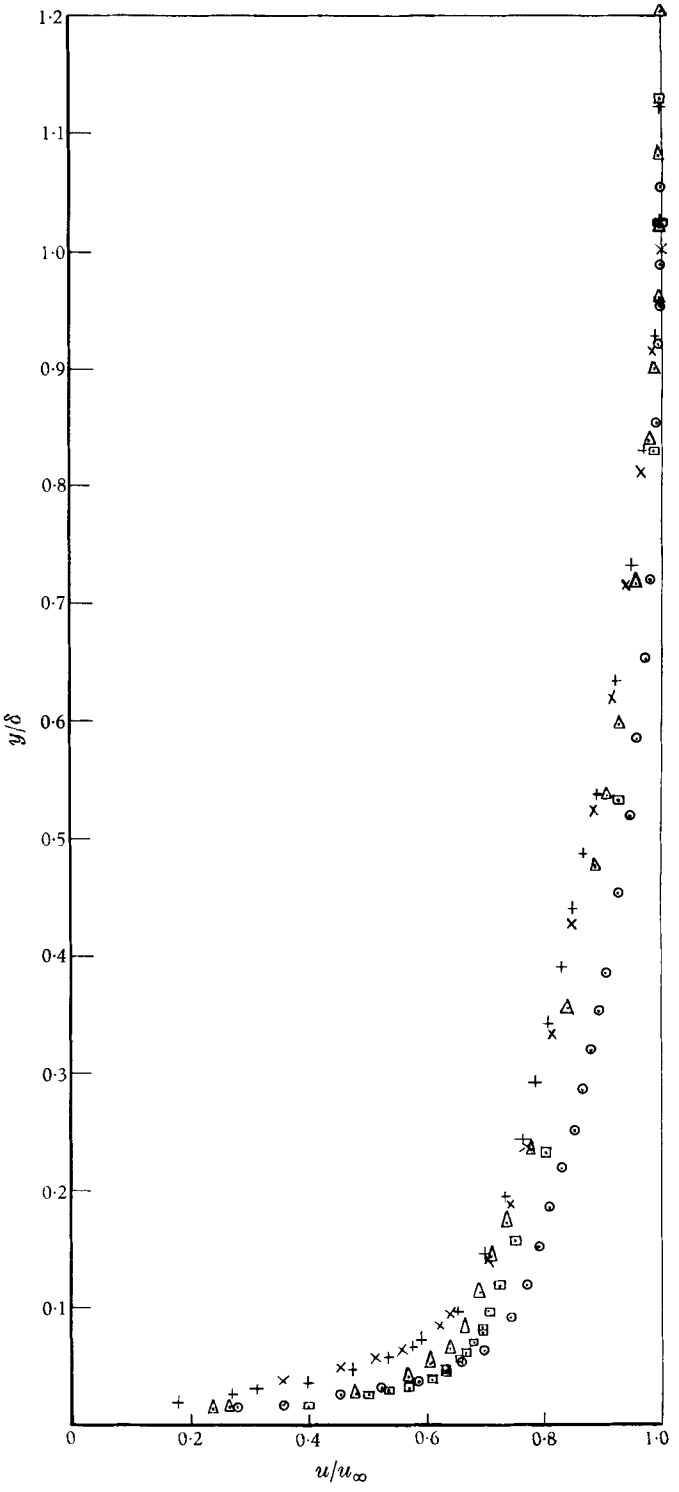

FIGURE 6. N.O.L. velocity profiles in physical co-ordinates. Key:

Symbol	M	$\frac{h_r - h_w}{h_r}$	Symbol	M	$\frac{h_r - h_w}{h_r}$
⊙	4·93	0	+	7·67	0·488
⊡	5·06	0·420	×	8·18	0·495
△	6·83	0·444			

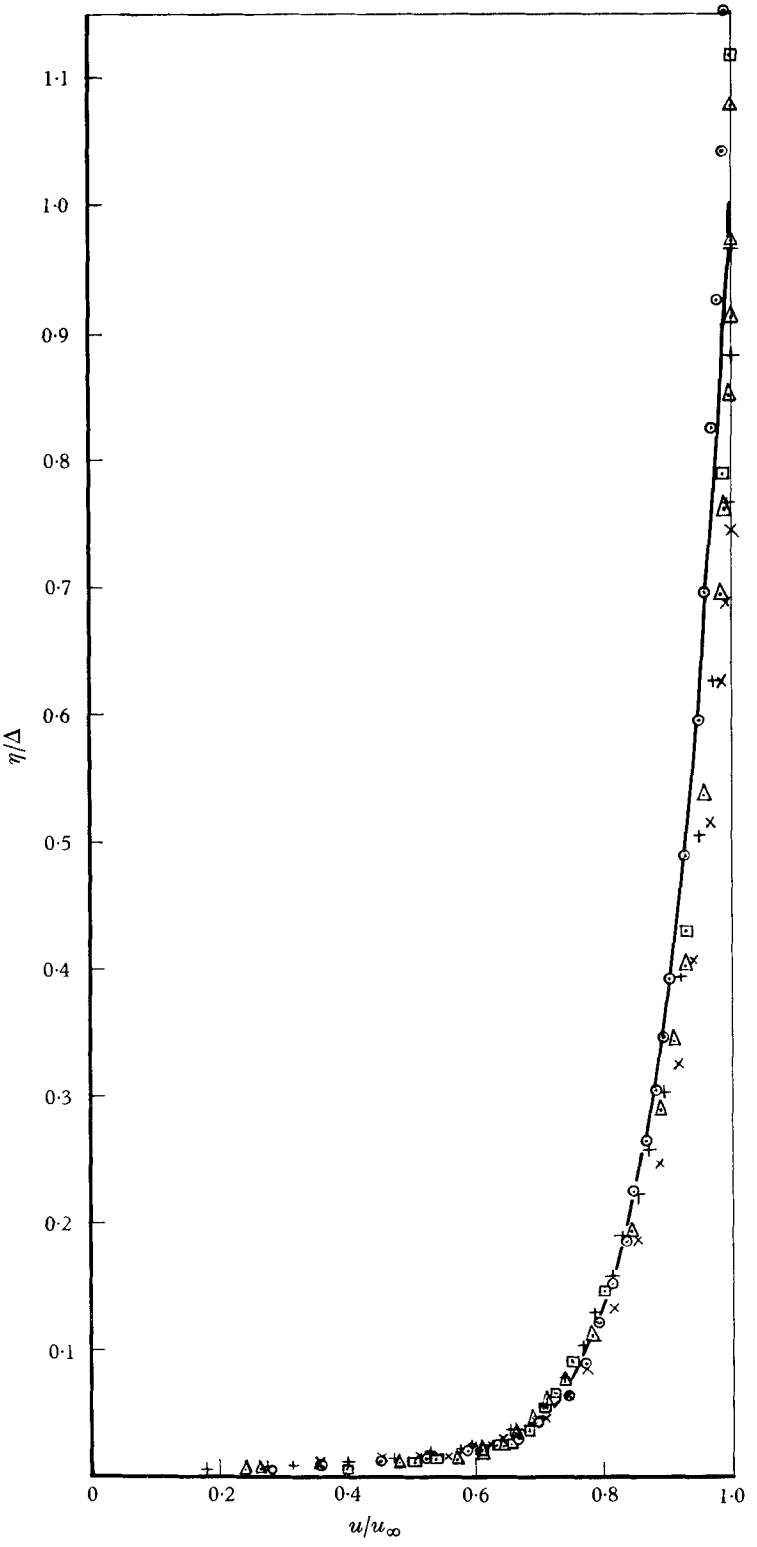

FIGURE 7. N.O.L. velocity profiles in transformed co-ordinates. Symbols as in Figure 6. ——, $u/u_\infty = (n/\Delta)^{\frac{1}{6}}$.

The values of $(u_\tau/u_\infty)^2$ so found agreed well with those published for the R.A.E. data, but with the N.O.L. data there were systematic discrepancies of up to 25 % in the cases with heat transfer. The values of c_f measured by the N.O.L. decrease with wall cooling, which is the opposite tendency to that predicted by the intermediate enthalpy theory. The measured values were obtained (*a*) from the measured heat-transfer rates, assuming the Reynolds analogy factor to be 1·2, and (*b*) from the slopes of the velocity profiles in the sublayer. Neither method is very reliable, and the theoretical values of skin friction corresponding to the

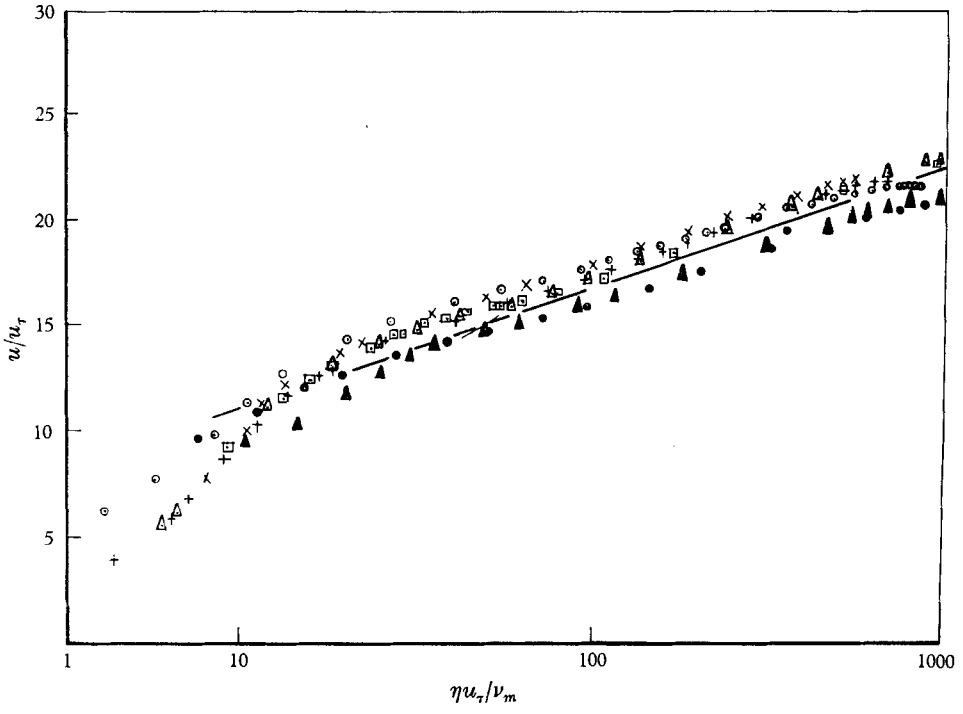

FIGURE 8. Inner behaviour of experimental velocity profiles. ——, $2{\cdot}5 \log (\eta u_\tau/\nu_m) + 5{\cdot}5$. R.A.E. data 13·4 station: ●, with heat transfer; ▲, zero heat transfer. Other symbols as for figures 6 and 7.

observed local Reynolds numbers were preferred in the present analysis to those quoted by Lobb *et al.*, since the bulk of other experimental work tends to support the intermediate enthalpy formula. The collapse to a single profile shown in figure 8 would not have been as complete if u_τ had been based on the quoted values of c_f, although the curves would still lie closer together than when plotted with y, ν_w and a wall-friction velocity $u_{\tau_w} = (\tau_w/\rho_w)^{\frac{1}{2}}$ in place of η, ν_m and u_τ, as in their paper.

There is a small but systematic discrepancy between the data from the two sources as plotted in figure 8, the N.O.L. points all lying a little above the standard curve $u/u_\tau = 2{\cdot}5 \log (\eta u_\tau/\nu_m) + 5{\cdot}5$ and the R.A.E. points somewhat below. This is almost certainly due in part to residual Mach number effects not removed by the transformation, the presence of which would be likely to show since Monaghan

& Cooke worked at about $M = 2$ and Lobb *et al.* at hypersonic speeds. The discrepancy may also reflect the fact that even to-day there is no general agreement among experimental workers on the precise values of the constants A, B in the logarithmic law (see, for example, Table 1.1 of the forthcoming volume *Incompressible Aerodynamics* edited by Thwaites, in which a number of sets of values from the literature are listed). The values $A = 2{\cdot}5$, $B = 5{\cdot}5$ used in this paper are probably the best known. The reason for this measure of disagreement may lie in the fact that some dependence on a Reynolds number such as $u_\infty \delta/\nu_\infty$ should strictly be included in the inner law; but in part no doubt it also arises from the difficulty of measuring skin friction accurately.

In a recent note Yasuhara (1959) has attempted a correlation of some experimental profiles in terms of a defect law of the form $(u_\infty - u)/u_\tau$ as a function of η/Δ. The fact that this was not very successful may also have been due to uncertainty about the skin friction.

7. Concluding remarks

From the evidence of figures 6 and 7 there seems little doubt that the method of collapsing the outer four-fifths or so of the velocity profiles as a function of η/Δ is valid, and this justifies *a posteriori* the calculations of the shear stress and enthalpy distributions in §§3 and 4. Other investigators have remarked on the fact that the index n in the approximating power law $(y/\delta)^{1/n}$ decreases with Mach number—as shown in figure 6—but this change in n is conveniently removed by the present transformation. This result, and the further fact that the enthalpy-velocity relation is approximately quadratic, can be used empirically to treat more complicated boundary-layer flows as well: for instance, the relation between the compressible and incompressible values H and H_i, say, of the form parameter δ^*/θ, is found from (2) and (41) to be

$$H = (h_w/h_\infty)\, H_i + (h_r/h_\infty) - 1, \tag{44}$$

and this equation has been used (Spence 1960) to calculate the growth of the boundary layer in a pressure gradient by an extension of the methods available for incompressible flow.

The uncertainty about the skin friction in the N.O.L. tests make the validity of the inner law (7) less certain than that of the outer law. One can certainly draw the more limited conclusion that if u_τ is defined from the value of τ_w predicted by equation (9), irrespective of whether this is correct, then u/u_τ is somewhere near the standard logarithmic function of $\eta u_\tau/\nu_m$ given by (7). This on its own, however, is not a very tidy result, for if $\rho_m u_\tau^2$ so defined were not in fact equal to the wall shearing stress, the profile in the sublayer could not be written $u/u_\tau = \eta u_\tau/\nu_m$ as in equation (5), and the reasoning leading to the functional form $u/u_\tau = g(\eta u_\tau/\nu_m)$ in the logarithmic region would no longer apply.

It was also assumed in deriving this expression that the density-viscosity law could be approximated for constant pressure by $\rho\mu = \text{constant}$, i.e. excluding effects of dissociation by $\mu \propto T$. This might at first sight seem to rule out hypersonic flows at the extreme stagnation enthalpies typical of re-entry. But the relation can always be taken in this form over a suitably restricted range of

temperatures, and as table 2 shows, the width of the range over which a single constant of proportionality could be used becomes surprisingly wide at high temperatures. The table is constructed from the results for dry air calculated by Hirschfelder *et al.* (1955). The assumption is clearly satisfactory for the temperatures between 100 and 300 °K covered by both sets of data analysed, and

T (°K)	100	200	300	500	1000	2000	3000	5000
$\mu/T \times 10^7$ (g/cm sec °K)	7·02	6·68	6·17	5·36	4·26	3·34	2·90	2·41

TABLE 2

should work moderately well, at least across the sublayer, to which the viscous effects are mainly confined even for wall temperature as high as 1000 °K. Since the viscosity enters the expression for skin friction only to a small power, this will not be greatly in error. But the use of the intermediate enthalpy formula would of course be highly speculative at such temperatures, and departures from the inner law might well become more marked. On the other hand, there is no particular reason to expect the outer law to break down at higher temperatures, since it does not depend on viscosity; but the conclusions drawn from it regarding the enthalpy distribution might be slightly modified by the variation of specific heat and Prandtl number.

REFERENCES

CLAUSER, F. H. 1956 *Advances in Applied Mechanics. IV*, **1**. New York: Academic Press.

COLES, D. 1956 *J. Fluid Mech.* **1**, 191.

CULICK, F. E. C. & HILL, J. A. F. 1958 *J. Aero. Sci.* **25**, 259.

ECKERT, E. R. G. 1955 *J. Aero Sci.* **22**, 585.

FALKNER, V. M. 1943 *Aircr. Engr.* **15**, 169.

HIRSCHFELDER, J. O., BIRD, R. B., CURTISS, C. F. & SPOTZ, E. L. 1955 Section D of *Thermodynamics and Physics of Matter* (Table D 7*d*) (F. D. Rossini, editor). Princeton University Press.

LOBB, R. K., WINKLER, E. M. & PERSH, J. 1955 *J. Aero. Sci.* **22**, 1.

MATTING, F. W., CHAPMAN, D. R., NYHOLM, J. R. & THOMAS, A. G. 1959 *Proc. Heat Trans. and Fluid Mech. Inst., Los Angeles*, p. 80.

MONAGHAN, R. J. & COOKE, J. R. 1953 *Aero. Res. Coun.* C.P. no. 140.

RANNIE, W. D. 1956 *J. Aero. Sci.* **23**, 485.

RUBESIN, M. W. 1953 *Nat. Adv. Com. Aeron., Tech. Note* 2917.

SEIFF, A. 1954 *Nat. Adv. Com. Aeron., Tech. Note* 3284.

SPENCE, D. A. 1951 *Aero Res. Coun. Rep.* 14162 (see also, *J. Aero. Sci.* 1956, **23**, 3).

SPENCE, D. A. 1960 *R. & M. Aero. Res. Coun., Lond.*, no. 3191.

SQUIRE, H. B. 1948 *Phil. Mag.* (7), **39**, 1.

VAN DRIEST, E. R. 1955 *Proc. Heat Trans. and Fluid Mech. Inst., Los Angeles*, paper XII.

VON KÁRMÁN, TH. 1921 *Z. angew Math. Mech.* **1**, 237.

YOUNG, A. D. 1953 *Rep. Coll. Aero. Cranfield*, no. 73.

YASUHARA, M. 1959 *J. Aero/Space Sci.* **26**, 528.